Title: Dynamics of ZnO laser produced plasma in high pressure argon

Authors: V.E. Kaydashev, J.G. Lunney

PII: S0169-4332(10)01704-6
DOI: doi:10.1016/j.apsusc.2010.11.181
Reference: APSUSC 21057

To appear in: *APSUSC*

Received date: 26-5-2010
Revised date: 11-10-2010
Accepted date: 26-11-2010

Please cite this article as: V.E. Kaydashev, J.G. Lunney, Dynamics of ZnO laser produced plasma in high pressure argon, *Applied Surface Science* (2010), doi:10.1016/j.apsusc.2010.11.181

This paper describes the results of some experiments to investigate the laser plume dynamics in the high gas pressure (5×10^3 - 10^4 Pa) regime used for PLD of ZnO nanorods. Time- and space-resolved UV/visible emission spectroscopy and Langmuir probe measurements were used to diagnose the plasma and follow the plume dynamics. By measuring the spatial profiles of Zn I and Zn II spectral lines it was possible to follow the propagation of the external and internal shock waves associated with the interaction of the ablation plume with the gas. The plume dynamics was also studied for ZnO targets doped with elements which are lighter (Mg), comparable to (Ga), and heavier (Er) than Zn, to see if there is any elemental segregation in the plume.

Dynamics of ZnO laser produced plasma in high pressure argon.

V. E. Kaydashev [1] *and J. G. Lunney*[2]

[1] *Mechanics and Applied Mathematics Research Institute, Southern Federal University, 344090, Rostov-on-Don, Russia.*
[2]*School of Physics, Trinity College Dublin, Dublin 2, Ireland.*

Contact: e-mail: kaidashev_mst@mail.ru

Abstract

Pulsed laser deposition of ZnO in high pressure gas offers a route for the catalyst-free preparation of ZnO nanorods less than 10 nm in diameter. This paper describes the results of some experiments to investigate the laser plume dynamics in the high gas pressure (5×10^3 - 10^4 Pa) regime used for PLD of ZnO nanorods. In this regime the ablation plume is strongly coupled to the gas and the plume expansion is brought to a halt within about 1 cm from the target. A 248 nm excimer laser was used to ablate a ceramic ZnO target in various pressures of argon. Time- and space-resolved UV/visible emission spectroscopy and Langmuir probe measurements were used to diagnose the plasma and follow the plume dynamics. By measuring the spatial profiles of Zn I and Zn II spectral lines it was possible to follow the propagation of the external and internal shock waves associated with the interaction of the ablation plume with the gas. The Langmuir probe measurements showed that the electron density was 10^9-10^{10} cm^{-3} and the electron temperature was several eV. At these conditions the ionization equilibrium is described by the collisional-radiative model. The plume dynamics was also studied for ZnO targets doped with elements which are lighter (Mg), comparable to (Ga), and heavier (Er) than Zn, to see if there is any elemental segregation in the plume.

Introduction

There is much interest in the development of reproducible techniques for the preparation of ZnO nanorods, and pulsed laser deposition (PLD) in a high pressure gas offers a catalyst-free route [1]. Since ZnO is a wide band gap semiconductor with a large exciton binding energy (63 meV), it is of interest for a range of UV applications. The possibility to change the band gap width, conductivity and emitting properties of ZnO by doping is critical for the design of new devices for nanophotonics, nanoelectronics and nanosensors. By doping with Mg (up to 20 wt. %) the band gap can be tuned from 3.3 to 3.8 eV [2]. ZnO:Ga_2O_3(0.5%) films have been prepared with resistivity as low as $3x10^{-3}$ ohm cm without degradation of crystal structure [2]. These films had high Hall mobility (μ~70 cm^2/Vs) and high transmission (~80%) in visible region of spectrum [2]. ZnO nanorods doped with Ga have yielded electron emission current density comparable to that obtained from carbon nanotubes [3]. ZnO:Er shows photoluminescence near 1.54 μm which is of interest for the development of optical waveguide devices. This photoluminescence of films can be enhanced by increasing the Er content up to 2 wt. % [4].

In PLD of ZnO nanorods it is of interest to investigate how the ablation plume interacts with the relatively high pressure (10^3 - 10^4 Pa) gas and how the plasma conditions influence the nanorod growth. In PLD the expansion of the laser ablation plume in vacuum has been investigated theoretically [5] and experimentally [6] for some metals and semiconductors. There are also several experimental [7] and theoretical [8,9] studies of laser ablation of metals and some oxides in gas. While there are some ZnO plume studies in thin film deposition conditions [10], it seems that the higher pressure regime used in nanorod deposition has not been investigated.

This paper reports the results of a study of the plume dynamics in laser ablation of ZnO in argon in the high pressure regime used for PLD of nanorods. By comparing data obtained from time- and space-resolved UV/visible emission spectroscopy and Langmuir probe measurements with theoretical models of plume expansion in gas [8,9] it is possible to gain some understanding of plume dynamics. The influence of doping with Mg, Ga and Er on electron temperature and plume stopping distance was also investigated.

Experiment

Pure ZnO and ZnO doped by Mg (20 wt. %), Ga (0.4 wt. %) and Er (1.75 wt. %) ceramic targets were prepared by mixing and pressing appropriate amounts of ZnO and MgO, Ga_2O_3 and Er_2O_3 powders respectively. The targets were sintered for 12 h in air at 1100 ºC. Laser ablation was done by focusing a KrF (248nm) laser beam on a rotating target to give a fluence of 2.5 J cm^{-2} on a 0.06 cm^2 elliptical spot. The vacuum chamber was evacuated down to 10^{-2} Pa and then filled up to 5×10^3 Pa or 10^4 Pa of argon. The main plasma diagnostic techniques were time- and space-resolved UV/visible emission spectroscopy and Langmuir probe measurements. For the spectroscopy an image of laser plume axis was formed on entrance slit of an Andor MS260i imaging spectrograph so that the plume axis (normal to target surface) lay along the slit. The spectrograph was equipped with a 300 lines per mm grating and a gated ICCD camera. The ICCD was triggered at a variable delay after the laser pulse and the gate time was 50 ns. The spectral resolution was 0.3 nm and the spatial resolution along the target normal was 140 μm. The Langmuir probe was 2×2 mm^2 copper plate insulated on one side and mounted at 6 mm from the target on axis of plume and lying parallel to plasma flow. The probe was biased as in Ref. [11]; the bias could be

negative to measure the ion current, or positive to measure the electron current, drawn from the plasma.

Results and Discussion

The dynamics of laser ablation plumes of pure ZnO, ZnO:Mg (20%), ZnO:Ga (0.4%) and ZnO:Er (1.75%) targets at 5×10^3 Pa and 10^4 Pa were investigated using time delays from 200 ns to 10 μs after laser pulse. Ion flux measurements were made at a bias voltage of -20 V, where the ion signal is fully saturated. For electron temperature and density measurements the IV characteristics were measured in the bias range 0 to 15 V. Langmuir probe theory, commonly used for calculation of electron temperatures of laser plasma in vacuum [12], was applied to individual peaks which appear in electron signal. By comparing the Langmuir probe and the time- and space-resolved UV/visible emission spectroscopy measurements it was possible to associate electron current peaks with the arrival of external and internal shock waves at the probe position.

Figure 1 shows the ion and electron probe signals for ablation of pure ZnO in 5×10^3 Pa of argon. Figure 2 shows the spatial profiles of the Zn I 481.0 nm line recorded at various time delays for both 5×10^3 and 10^4 Pa of argon. From these profiles it can be seen that at 5×10^3 Pa the forward motion of the plume comes to a halt at ~9 mm from the target and the contact surface of external shock wave reaches the probe position (6 mm) at ~800 ns after laser pulse. This time corresponds to the appearance of the second peak in the electron signal (Fig.1 (b)). When argon pressure is increased from 5×10^3 to 10^4 Pa, the stopping distance is ~7 mm, though the main features in the probe a spectroscopy signal are quite similar. Only the results of measurements at 5×10^3Pa will be considered in detail here.

The first peaks in ion (280 ns) and electron (200 ns) signals (Fig. 1) correspond to plasma transmitted through the gas without collisions [7]. The external shock wave reaches the probe at t_2=800 ns. A broad spectral line at 491.8 nm, which is assumed to consist of two lines Zn II at 491.2 nm and 492.4 nm, disappears from spectra for times later than ~2 μs after laser pulse. At 5×10^3 Pa of argon the forward motion of the ZnO plume front is halted at ~1.8 μs. At this time the maximum of the Zn I 481.0 nm emission is at ~6 mm and the emission falls to 10% of maximum at ~8 mm, (Fig. 2(a)). Figure 3 shows the temporal evolution of the position of the maximum of 481.0 nm line and the positions at the inner and outer 10 % levels for both the pure ZnO and the doped targets. The moment when plasma stops corresponds to the time when external shock wave in argon stops (Mach number of external shock wave becomes equal to 1). Thereafter the internal shock wave in plume starts moving back towards the substrate. It should be mentioned that an internal shock wave is quite weak and looks somewhat like a relaxation matter wave. It reaches the probe position at t_3=2400 ns and the third peak of electron signal is observed (Fig. 1(b)). As can be seen in Fig. 2 and 3, at ~4 - 6 μs the internal wave in plume is reflected at a distance of ~ 0.2 - 1 mm from the target and decays as it moves slowly towards the position where the plume is first halted. This feature was observed for pure and doped targets (Fig. 3). It can be seen that there is a rather good correlation between the spectroscopy measurements and the electron current signals measured by the probe. Thus it seems that a Langmuir probe detecting electrons is a useful device for investigating shock wave dynamics associated with laser ablation in a background gas.

The measurements reported here seem to show some qualitative differences from earlier studies of ablation plume expansion in gas ambient pressure of 10^5 Pa [9] and 10-10^3

Pa [8]. In case of high pressure [9] the strong internal shock wave was twice reflected from the target, whereas at low pressure [8] the plasma was considered to be homogenized when internal shock wave reaches the center of a plume. It can be seen from Fig. 3 that the plume is brought to a complete halt in 8-10 μs and the probe lies in the region of strong spectral line emission. Thus, it can be concluded that the fourth broad peak of electron current is due the regime the plume expansion has been halted and is homogenized.

Having identified how the peaks in the electron signals are due to the arrival of the contact surfaces of external shock wave and internal shock wave at the probe position, the bias dependence of the electron signals can be used to find the electron temperature. Langmuir probe theory is commonly applied for measurement of plume electron temperature for laser ablation in vacuum where only one sharp peak is observed [12]. To our knowledge, probes have not so far been used to measure electron temperature and density within in shock waves formed by laser ablation in gas. The values electron temperature and density at t_2=800 ns and t_3=2400 ns for the ZnO plume at 5×10^3 Pa are shown in Table 1. The contact surface behind external shock wave had electron temperature of 1.8 eV and electron density of 3.5×10^9 cm^{-3}. By the time when the plume has been brought to a halt the part of the kinetic energy due to plasma flow is transformed to thermal energy. The internal shock wave, moving back to the substrate, continues to heat the plume. As it moves past the probe surface (6-8 mm from the target) the measured electron temperature is found to be 2.6 eV and the density was 1.7×10^9 cm^{-3}. The electron temperature at the time of maximum electron current (24 μs) from the homogeneous plume was 0.9 eV.

For PLD of doped nanorods it is of interest to know if the plume stopping distance depends on the nature and concentration of the dopant. Thus, using the methods described above, the plume dynamics was measured for ZnO doped with Mg (24.3 amu), Ga (69.72 amu) and Er (167.26 amu). Ga has about the same atomic weight as Zn (65.37 amu), while Mg is lighter and Er is heavier. The values of molar masses were calculated to be 81.36, 81.31, 69.95 and 82.86 g/mol for ZnO, ZnO:Ga(0.4 wt.%), ZnO:Mg(20 wt.%) and ZnO:Er(1.75 wt.%) respectively. The dynamics of pure and doped ZnO plumes, as measured by the spatial distribution of the Zn I 482.0 nm line, is shown in Fig.3. It seems that doping with 1.75% of Er give rise to a small but detectable increase in the stopping distance as compared to pure ZnO, while doping with 20% of Mg reduces the stopping distance by 10-15%. These variations are of interest in terms of choosing the optimal target-substrate distance in nanowire PLD. The space-resolved spectroscopy showed that the spatial distributions of ZnI and MgI, GaI, ErI spectral lines were all quite similar, indicating that stoichiometric transfer of doping atoms should be possible to distances of the order of the of the stopping distance. Figure 3(e) shows graphs of the position vs distance of the maxima Zn I 481.0 nm line distributions for the ZnO and doped ZnO plumes. By fitting these graphs with second order polynomials of the form $Z(t) = Z_0 + V_0 t - at^2/2$, the initial velocities (V_0) and decelerations (a) can be found, and are shown in Table 1. It should be pointed out that this fitting is possible only for time delays greater that ~500 ns after laser pulse. It can be noted that the ZnO:Mg(20%) plume shows the lowest value of initial velocity (4×10^3 m s^{-1}) and deceleration (190×10^7 m s^{-2}).

The electron temperatures and densities were determined at the peaks of the electron current, i.e. when the contact surface behind external shock wave (t_2=800 ns) and internal

shock wave in plume (t_3=2400 ns) reach the probe. These are presented in Table 1 for the various targets used. In case of ZnO:Mg(20%) target external shock wave stops close to probe position (maximum of Zn I spectral emission distribution stops at ~5.5 mm from the target) and only 2 peaks are observed in ion and electron signals. Comparing the electron temperatures of pure and doped ZnO plumes indicates that doping leads to a higher temperature plume. At this stage it is not clear why doping leads to an increase of the electron temperature. However, it seems possible that doping will lead to a change in the absorption coefficient at the laser wavelength for both the solid target and the vapor evolved during the laser pulse, leading to a change in the energy per particle in the early plume. The dopant concentrations considered in present paper were mainly chosen on the basis of practical application. To properly analyse the influence of different dopants on electron temperature and stopping distance, it will be necessary to investigate an ablation of plumes with equal concentrations of different dopants. The Langmuir probe measurements showed that the electron density was 10^9-10^{10} cm^{-3} and the electron temperature was several eV for all investigated targets. At these conditions the ionization equilibrium is described by the collisional-radiative model [13].

Conclusions

Laser plume dynamics in the high gas pressure (5×10^3 Pa and 10^4 Pa) regime used for PLD of ZnO nanorods was investigated. It is possible to identify the main features of the shock wave dynamics from the electron signals registered on a Langmuir probe. These signals were used to measure the electron temperature and density in the plume. Time-resolved measurements of the spatial distribution of the Zn I 481.0 nm emission can be correlated with the Langmuir probe signals. Doping the ZnO target seems to give enhanced heating of

the plume. The spatial distributions of the line from Zn I and Mg I, Ga I and Er I are all quite similar indicating that stoichiometric material transfer of doping atoms should be possible up to distances equal to the stopping distance.

Acknowledgements

The work was supported by Development of Higher School Science Potential, Russia (Project No. 2.1.1.6758/2009-2010) and by the Science Foundation Ireland Research Frontiers Programme of under project PHY2422.

References

[1] V. E. Kaydashev, E. M. Kaidashev, M. Peres, T. Monteiro, M. R. Correia, and N. A. Sobolev, Optical and Structural Properties of ZnO Nanorods Grown by Pulsed Laser Deposition without a Catalyst, Tech. Phys., 54 (2009) 1607-1611.

[2] M. Lorenz, E. Kaidashev, H. Wenckstern, V. Riede, C. Bundesmann, D. Spemann, G. Benndorf, H. Hochmuth, A. Rahm, H.C. Semmelhack, Optical and electrical properties of epitaxial $(Mg,Cd)_xZn_{1-x}O$, ZnO, and ZnO:(Ga,Al) thin films on c-plane sapphire grown by pulsed lased deposition, Sol. St. El., 47 (2003) 2205-2208

[3] X. Sun, Designing efficient field emission into ZnO, SPIE, 10.1117/2.102.0101(2006) 1-4

[4] L. Douglas, R. Mundle, R Konda, C. E. Bonner, A. K. Pradhan, D. R. Sahu, and J. L. Huang, Influence of doping rate in Er^{3+}:ZnO films on emission characteristics, Opt. Lett., 33 (2008) 815–817

[5] S. I. Anisimov, B. S. Luk`yanchuk, A. Luches, An analytical model for three-dimensional laser plume expansion into vacuum in hydrodynamic regime, Appl. Surf. Sci. 96-98 (1996) 24-32

[6] B. Toftmann, J. Schou, J. G. Lunney, Dynamics of the plume produced by nanosecond ultraviolet laser ablation of metals, Phys. Rev. B. 67 (2003) 104101-1-104101-5

[7] S. Amoruso, J. Schou, J. G. Lunney, Multiple scattering effects in laser ablation plume, Europhys. Lett. 76 (2006) 436-442

[8] N. Arnold, J. Gruber, J. Heitz, Spherical expansion of the vapor plume into ambient gas:an analytical model, Appl. Phys. A. 69 (1999) 87–93

[9] S. B. Wen, X. Mao, R. Greif, and R. E. Russo Expansion of the laser ablation vapor plume into a background gas. I. Analysis, J. Appl. Phys. 101 (2007) 023114-1- 023114-13

[10] K. J. Saji, N. V. Joshy, and M. K. Jayaraj, Optical emission spectroscopic studies on laser ablated zinc oxide plasma, J. Appl. Phys. 100 (2006) 043302-1-043302-5

[11] D.W. Koopman, Langmuir Probe and Microwave Measurements of the Properties of Streaming Plasmas Governed by Focused Laser Pulses, Phys. Fluids 14 (1971) 1707-1716

[12] B. Doggett, J. G. Lunney, Langmuir probe characterization of laser ablation plasmas, J. Appl. Phys. 105 (2009) 033306-1-033306-6

[13] T. Fujimoto, Kinetics of Ionization-Recombination of a Plume and Population Density of Excited Ions. IV. Recombining Plasma – Low-Temperature Case, J. Phys. Soc. J. 49 (1980) 1569-1576

Table 1 Electron temperatures and densities in external shock wave contact surface (peak 2) and internal shock wave (peak 3) of ZnO, ZnO:Mg(20%), ZnO:Ga(0.4%), ZnO:Er(1.75%) plumes. Also shown are the coefficients obtained by quadratic fitting the equation of motion maximum intensity at 5×10^3 Pa of argon.

	Peak 2 at 800ns		Peak 3 at 2400ns				
	T_e, eV	$N_{e,}$ cm^{-3}	T_e, eV	$N_{e,}$ cm^{-3}	X_0, μm	V_0,10^3m/s	a, 10^7m/s^2
ZnO	1.8	3.5×10^9	2.6	1.7×10^9	1800	4.6	230
ZnO:Mg(20%)	5	0.57×10^9			1700	4.0	190
ZnO:Ga(0.4%)	3.0	2.8×10^9	4.8	1.0×10^9	1000	6.6	350
ZnO:Er(1.75%)	3.0	2.5×10^9	3.7	0.84×10^9	1400	5.3	250

List of figure captions.

Fig.1 Ion (a) and electron (b, c) probe currents for ZnO plume in argon (5×10^3 Pa) at different bias voltages (probe is parallel to the plume axis and positioned at 6 mm from target).

Fig.2 Spatial distribution of Zn I 481.0 nm line emission along plume axis at 5×10^3 Pa (a,b) and 10^4 Pa (c,d) argon at different times after laser pulse.

Fig.3 Laser plasma plume dynamics for ablation of ZnO (a), ZnO:Ga(0.4%) (b), ZnO:Mg(20%) (c) and ZnO:Er(1.75%) (d) targets in 5×10^3 Pa of argon. The graphs show the position vs time of the maximum (squares) of ZnI 481.0 nm emission and of the inner (circles) and outer (triangles) 10% emission levels. Quadratic fitting of equation of motion of the position of maximum emission for the various target compositions is shown on panel (e).

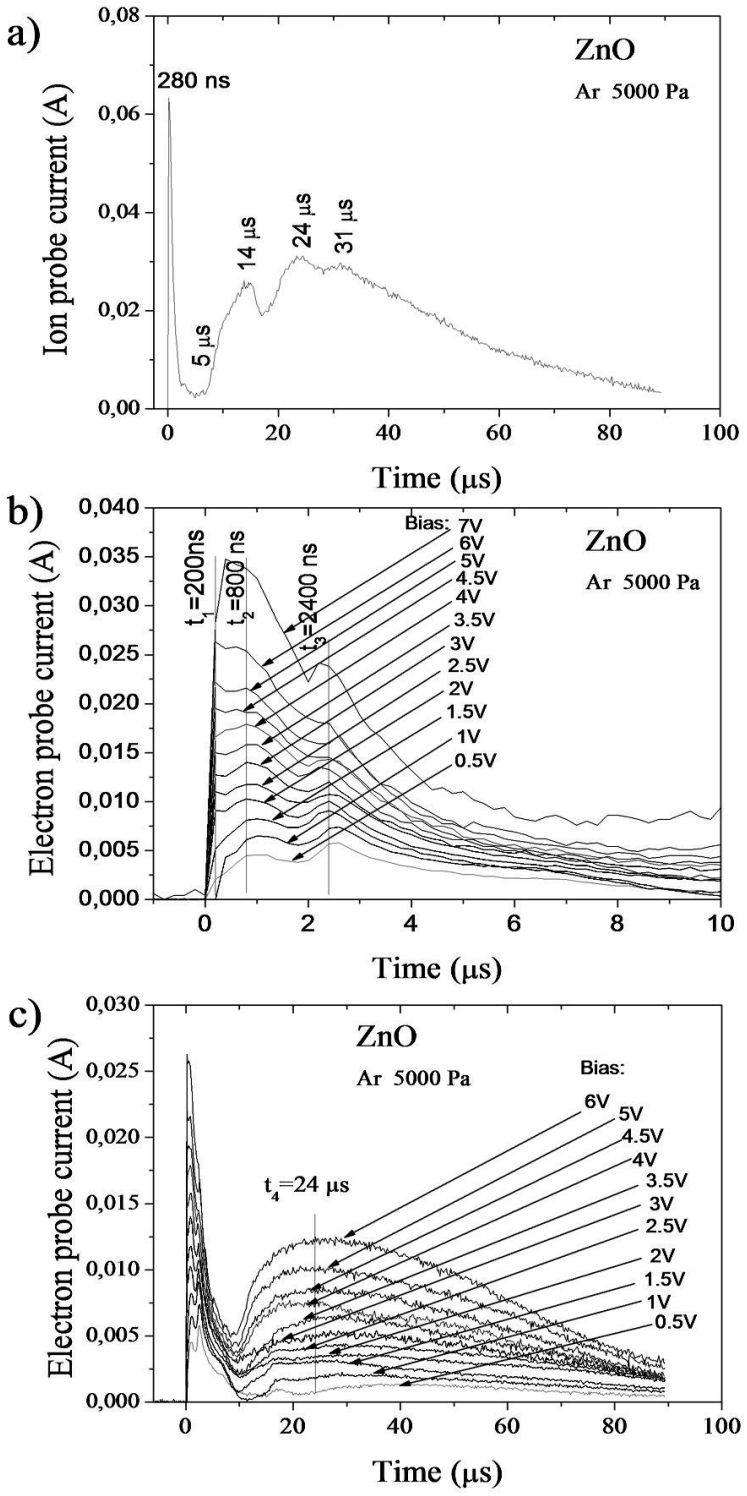

Fig. 1

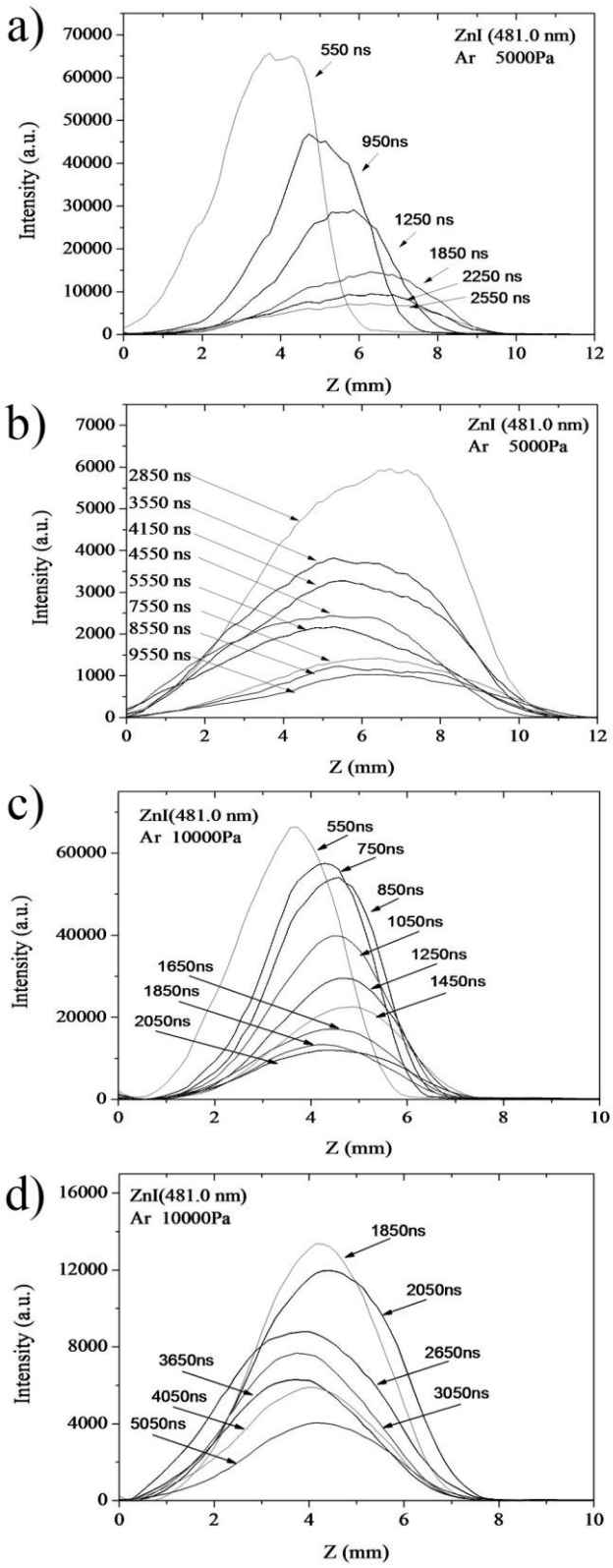

Fig.2

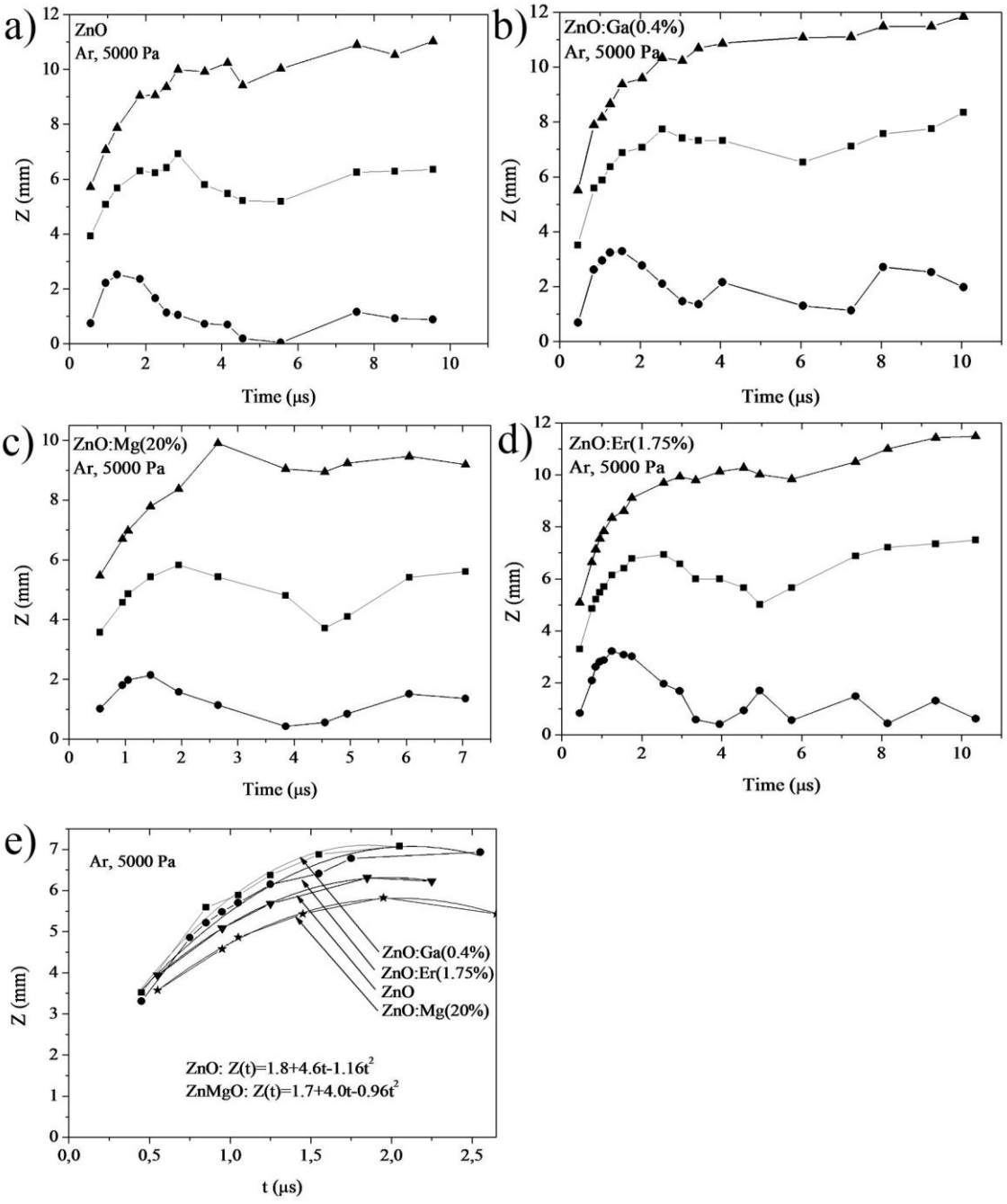

Fig.3